The footprint of an ancient forgotten earthquake: a VI Cent. A.D. event in the European Western Southern Alps.

Franz A. Livio[1], Maria F. Ferrario[1], Elisa Martinelli[1], Sahra Talamo[2], Alessandro M. Michetti[1], Silvia Cercatillo[2]

[1] Università degli Studi dell'Insubria, Dipartimento di Scienza ed Alta Tecnologia, Via Valleggio, 11, 22100 Como (CO) – Italy.

[2] University of Bologna, Alma Mater Studiorum, Department of Chemistry G. Ciamician, BRAVHO Radiocarbon Laboratory, Via Selmi 2, 40126, Bologna (BO) – Italy

Corresponding Author: Franz A. Livio franz.livio@uninsubria.it

Abstract

Low-deforming regions are characterized by long earthquake recurrence intervals; thus, it is fundamental to extend back as much as possible the record of past events. Evidence from single sites or proxies may be not compelling, whereas a more substantial picture may be obtained from the integration of paleo- and archaeo-seismic evidence at multiple sites, eventually supplemented with historical chronicles.

Here, we document deformations observed in a stratigraphic sequence (i.e., Via Manzoni Site) and in an archaeological site (Roman Baths) in the city of Como (N. Italy). We perform stratigraphic and sedimentological analyses on the sedimentary sequences at via Manzoni and we document Earthquake Archaeological Effects at the Roman Baths by means of Structure from Motion and field surveys. We interpret the observed deformations as due to earthquake ground shaking and provide constraints on the lower threshold for the triggering of such evidence. Radiocarbon datings and chronological constraints from the archaeological site allow to bracket the time of occurrence of the deformations at the VI century AD.

We move toward a more regional view to infer possible seismogenic sources by exploiting a dataset of published paleoseismic evidence in Swiss and N. Italy lakes. We perform an inverse grid search to identify magnitude and location of an earthquake that can explain all the positive and negative evidence consistent with the time interval of the event dated at Como.

Our results show that a so far undocumented earthquake (minimum Mw 6.32) with epicenter located at the border between Italy and Switzerland may account for all the observed effects. Our study calls for the need to refine the characterization of the local seismic hazard, especially considering that this region seems unprepared to face the effects of a potential earthquake similar to the VI century AD one.

Short Summary

We here document the occurrence of an ancient earthquake occurred in the European Western Southern Alps in the VI Cent. A.D. The analysis of the effects due to earthquake shaking in Como City (N Italy) and the comparison with dated offshore landslides in the Alpine lakes allowed us to make an inference on the possible Magnitude and the location of the seismogenic source for this event.

This study shed a light on an old seismic event that happened in an area characterized by rare moderate earthquakes, still posing a significant hazard to the territory.

1. Introduction

40   Italy has one of the most complete and accurate historical seismic catalogues in the world, that can be considered as complete for the last ca. 700 years for Mw ≥ 6.5 in NW Italy (Rotondi and Garavaglia, 2002; Stucchi et al., 2004). Nonetheless, it is well known that ancient events (i.e., older than medieval times) can be hardly accurately recorded by historical sources and that the probability of incompleteness grows with age (Guidoboni et al., 2005). This is mostly true in settings where chronicles are clustered in a few cities and where human and natural events had possibly destroyed the
45   records (Guidoboni et al., 2005) or where well-preserved ancient archeological remains are sparse (e.g., high mountain sectors in the core of the European Alps). In regions characterized by low deformation rates, an exceedingly long earthquake recurrence interval could possibly imply a lack of information regarding the strongest events, with a significant underestimation of the seismic hazard. Thus, the recognition of ancient and prehistoric seismic events is essential for understanding the regional seismic potential of such regions.

50   Instead, natural records can be effective in filling the apparent gap in seismicity for ancient times. Some of the best examples are reported in studies on lake sediments, potentially able to image lake floor faulting or, more frequently, record large earthquakes as earthquake-triggered landslides / turbidites (e.g., Kremer et al., 2017, 2020; Oswald et al., 2021; Strasser et al., 2006, 2013). In the latter case, a paleoseismological significance of such evidence is inferred from the synchronicity of landslide events and by the spatial clustering in a certain region (Kremer et al., 2017). Nonetheless,
55   the earthquake-triggering and its age remains questionable or debated if age depth models are flawed and considering that mass wasting events can also be triggered by climatic causes as well (Borgatti and Soldati, 2010; Trauth et al., 2003). Additional constraints for a possible seismic triggering, would ideally be furnished by onshore evidence that are less prone to concurrent triggering by other causes and the consistency of both onshore and offshore data would provide an ideal integrated set of evidence for seismic triggering.

60   In this work, we present evidence from two sites in Como downtown, namely soft-sediment deformations in a stratigraphic sequence and disturbances in an archaeological site. Then, we look for coeval evidence, interpreted as paleoseismic, in lakes of the Western Southern Alps. This allows to provide a new hypothesis on the possible location of the seismogenic source and on the magnitude of the paleoearthquake.

2. Geological Setting

2.1. Regional seismotectonics and historical seismicity

The city of Como is located at the margin of the European Western Southern Alps, a sector of the Alps retro-wedge, bounded to the north and to the west by segments of the Periadriatic Lineament (Castellarin et al., 2006; Schmid and
70   Kissling, 2000).

This area has been actively involved into the collisional phase of the Alpine orogeny since the Cenozoic (Castellarin et al., 2006; Handy et al., 2010; Scaramuzzo et al., 2022; Zanchetta et al., 2015) up to recent times (e.g., Michetti et al., 2012; Sileo et al., 2007). To the south, the active front of the Southern Alps fold and thrust belt lies presently buried

beneath the Po Plain, facing the external arc of the Apennines with a relatively undeformed foreland in between the two chains (Fantoni et al., 2004; Scaramuzzo et al., 2022).

Across the western Southern Alps, shortening and seismicity rates significantly decrease westward (Figure 1). Moderate seismic events hit the Alps' innermost sectors during historical and early instrumental times, clustering to the NW of the area, mainly in the Valais region (i.e., the Sept. 3rd, 1295 Churwalden eq. Mw 6.2; the Dec. 9th, 1755 Brig-Naters eq. Mw 5.7; the 1855 Visp seismic sequence, max Mw 6.2; the Jan. 1946 Sierre seismic sequence, max. Mw 5.8; Rovida et al., 2016).

Other moderate historical events clusters are located along the pedemountain sector of the Southern Alps, including the strongest events that hit the whole Western Southern Alps and that can be regarded as the reference earthquakes for the whole region (the Dec. 25th, 1222 Brescia eq. Mw 5.68; the Nov. 26th, 1396 Monza eq. Mw 5.33; the May 12th, 1802 Valle dell'Oglio eq. Mw 5.6; Rovida et al., 2016). The historical catalogues do not report any pre-medieval earthquake in the region.
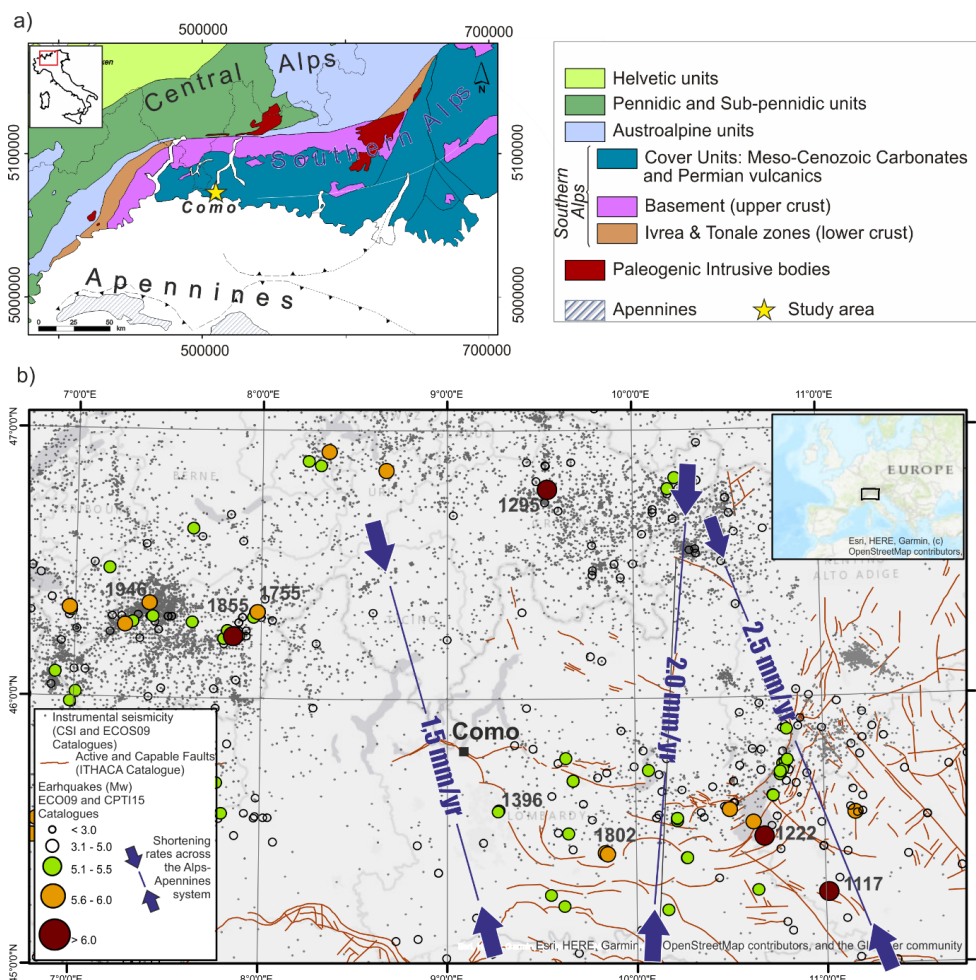
FIGURE 1: Geologic and seismotectonic setting for the study area: a) geological sketch map of the Southern Alps; b) seismotectonic setting: instrumental (ISIDe and ECOS09; **Fäh et al., 2011; ISIDe Working Group, 2007**) and historical (**CPTI15 AND ECOS09; FÄH ET AL., 2011; ROVIDA ET AL., 2016**) earthquakes are indicated; Active and capable faults after the ITHACA database (**Guerrieri et al., 2015; https://www.isprambiente.gov.it/en/projects/soil-and-territory/italy-hazards-from-capable-faulting-1?set_language=en**); shortening rates across the Alps-Apennines system are from **MICHETTI ET AL. (2012).**

Despite the relatively low rates of strain and seismic release, in the surroundings of the city of Como (Figure 1), other sparse geological and geomorphological clues for a recent seismic activity are reported, including both onshore (Michetti et al., 2012; Sileo et al., 2007) and offshore evidence (Fanetti et al., 2008; Kremer et al., 2020).

2.2. The Como urban area: geological and geomorphological setting, history and study sites

The Como urban area lies in a flat region at the end of the SW branch of Lake Como (Figure 1); the plain is bordered by bedrock mountain slopes, comprising Mesozoic pelagic limestones (Medolo Gr., Early Jurassic; Figure 2) to the NE, and deep sea turbiditic conglomerates and sandstones (Gonfolite Gr., Oligo-Miocene) to the SW (Michetti et al., 2014). The Gonfolite Backthrust is a N-verging tectonic structure putting in contact the Mesozoic succession with the younger

100   Gonfolite Group. Recent activity is documented by deformed Pleistocene to Quaternary sediments (Bernoulli et al., 1989; Sileo et al., 2007); in the Como urban area the fault was recognized during building excavations at Borgovico site (Figure 2); here, reverse surface faulting along a secondary splay of the Backthrust involves Late Pleistocene to Holocene sediments (Livio et al., 2011).

  The Cosia and Valduce creeks drain the plain, reaching Lake Como in the E and W sectors of the urban area, respectively;
105   today, the final part of their course is buried beneath the city. The Como branch of the lake is hydrologically closed, since the only outlet is the Adda River, which outflows from the Lecco branch. During the Quaternary, the region was repeatedly occupied by glaciers. Given the local geomorphological setting and landscape evolution, the subsoil of the Como plain is composed of a sequence of fine, loose materials of lacustrine and fluvial origin, deposited since the Late-glacial and throughout the Holocene; the environmental evolution of the study area has been reconstructed by means of stratigraphic,
110   geotechnical and hydrogeological data, macro-remains and pollen analyses, and radiocarbon dating (e.g., Comerci et al., 2007; Ferrario et al., 2015; Martinelli et al., 2017).

  The sedimentary sequence is composed, at the base, of inorganic clays settled in a proglacial lake following the last deglaciation. The lake level lowered progressively, allowing the development of a palustrine-lacustrine environment; this phase is attested by a thick sequence of sandy silts rich in organic remains (maximum thickness exceeds 40 m in the
115   depocenter of the basin). During the Holocene, the basin was filled by alluvial deposits of the Cosia and Valduce creeks; the shallowest stratigraphic unit is constituted by 1-10 m of reworked materials, historical in age.

  The presence of organic silts is the predisposing factor of the subsidence phenomena affecting Como town (Nappo et al., 2020). Subsidence rates are higher toward the lakeshore and at the center of the basin; due to groundwater overexploitation, subsidence reached critical rates (few cm/yr) in 1950-1970s; water extraction is forbidden since 1980
120   and today subsidence goes on at rates of few mm/yr, locally threating the historical buildings (Nappo et al., 2021).

  The oldest human occupation in the Lake Como area dates back to 60-50.000 cal yr BP, as suggested by sparse findings of worked flints (Cremaschi, 2000); a more widespread occupation since the Mesolithic is documented at several sites, either in the lowlands and surrounding mountains (Casini, 1994; Castelletti and Motella De Carlo, 2012; Martinelli et al., 2017; Uboldi, 1993). During the Iron Age, the hills surrounding the Como plain were stably inhabited (Martinelli et al.,
125   2022; Uboldi, 1993), while the plain itself was occupied by a marsh and thus not suitable for human occupation. The plain is in a strategic position for trade along S-N routes, connecting the Po Plain and the rest of Italy with Northern Europe; thus, the plain was reclaimed and in year 59 BC Julius Caesar founded *Novum Comum*, the first settlement in nowadays Como urban area (Luraschi, 1997). Human interventions deeply modified the local environment, including the diversion of the Cosia creek. The coastline position progressively moved from S toward N, firstly due to sediments supplied by the
130   rivers, and later due to anthropic land reclamation (Figure 2a-b). Since the occupation of the plain, the local evolution is the result of the interplay among natural processes and human control.

  Archaeological findings are widespread in the Como urban area (Uboldi, 1993) and here we focus on two sites, namely via Manzoni (Via Manzoni Site, hereafter) and the Roman Baths (Figure 2b; Jorio, 2011), where archaeo- and paleoseismic evidence has been discovered.

135   The Roman Baths have been unearthed in 1971 and then new excavations have been completed in the early 2000's. The latest excavations at the Roman Baths were conducted in 2009 under the scientific supervision of the Archaeological Superintendence (Scientific Director: Dr. Stefania Jorio). The archaeological site occupies more than 1500 m^2 and

includes several edifices and a central courtyard, interpreted as the Roman Baths of the town. Two building phases have been identified (Figure 3b): the oldest dates back to the second half of the 1st century AD, and the later one to the 2nd century AD. An abandonment and dismantling phase occurred in the 4th century AD is testified by a layer of alluvial deposits covering a ruin layer; the site was re-used in 5th- 6th century AD as a burial place and finally covered by alluvial sediments.

At Via Manzoni Site, excavations were carried out in 2016 at a building site (Scientific Director: Dr. Lucia Mordeglia). Here, we could analyze the 3D setting of a 9-m thick sedimentary sequence, exposed in different sections.
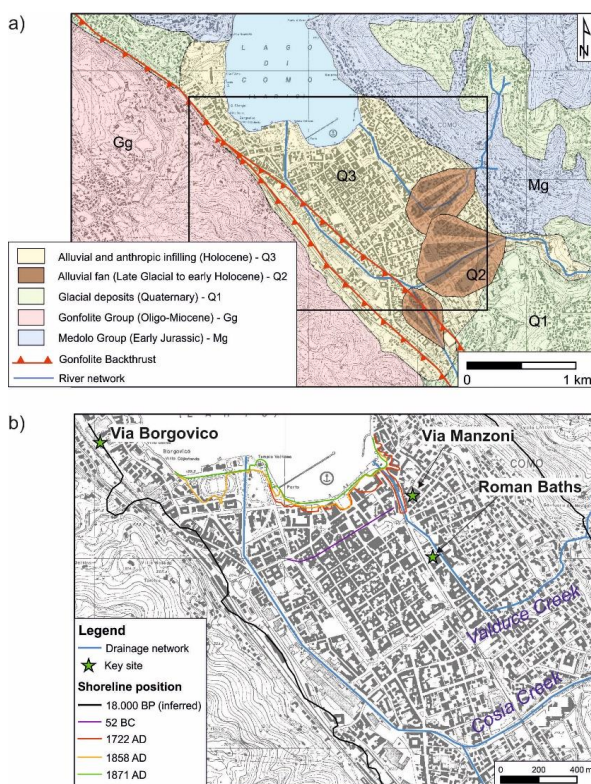
Figure 2: a) Simplified geological and geomorphological setting of Como area (modified after Michetti et al., 2014). B) River network and coastline position at different times (modified after Ferrario et al., 2015); basemap CTR (Carta Tecnica Regionale; 1:10,000 scale), after Regione Lombardia *Viewer Geografico 2D - Geoportale (servizirl.it).*

3. Methods and Materials

3.1. Stratigraphy and sedimentological analysis

We here provide a detailed description of some stratigraphic sections exposed by building excavations in the downtown Como area, at the Via Manzoni Site. The location excavations and the geometry and location of the outcropping sections, described hereafter, is given in Figure 2. Excavations exposed a grid of vertical sections, from the depth of 3 meters below ground level (BGL) down to 9 meters BGL. These sections provided a detailed stratigraphy covering the pre-Roman to historic time window in the shore environment of Lake Como. The detailed description of the Sections is given in the Supplementary Material.

We defined each stratigraphic unit based on the macroscopic characteristics in terms of texture, fabric, grain size distribution, petrography and content in macroscopic biological remains and/or archeological ones. Unconformities and erosive surfaces have also been considered, if well-recognizable in the field.

160
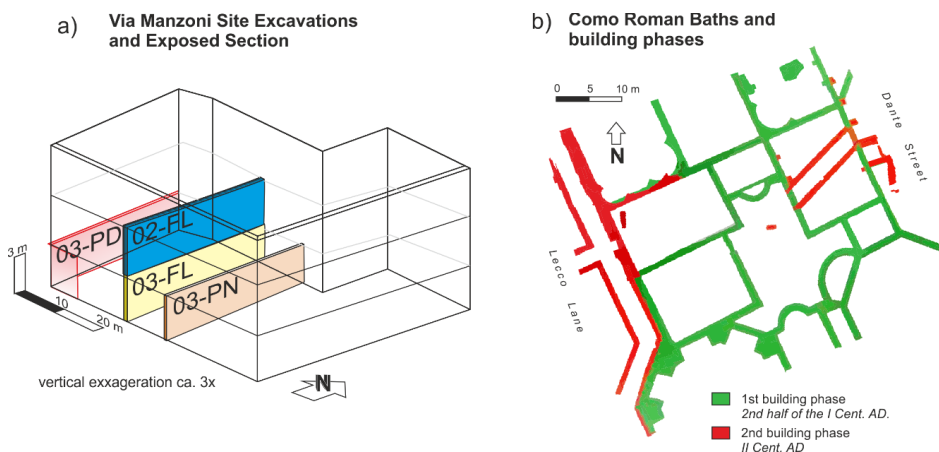
Figure 3: a) three-dimensional fence diagram with the location of the analyzed stratigraphic sections (codes are reported) – see the Supplementary Material for a detailed description of each section; b) map of the Como Roman Baths with indications of the building phases (modified after Jorio, 2011).

3.2. Radiocarbon dating (14C)

165

We selected 13 wood samples from Via Manzoni site for radiocarbon dating. They were pretreated at BRAVHO laboratory at Bologna University and the cellulose was extracted following the procedure tested in (Cercatillo et al., 2021). The BABAB (Base-Acid-Base-Acid-Bleaching) protocol includes an initial overnight bath in 5% NaOH, which cleans the sample from humic acids. The following steps include acidic (HCl 4%) and alkaline (NaOH 4%) solutions and a final bleaching in 5% $NaClO2$. The entire procedure is carried out at 70°C. When possible, at least 70 mg of wood was sampled (Table 1). Once the cellulose was dry (Table 1), an aliquot of 2,5 – 3 mg was put in aluminum cups and sent to MAMS radiocarbon laboratory for graphitisation and radiocarbon age determination. During the pretreatment two samples completely dissolved and for other two the quantity of extracted cellulose was not sufficient for dating. Analysis of the archeoseismological evidence

170

175

We investigated the deformations and damages still preserved in the unearthed Roman Baths of the city of Como (Figure 2 for the location).

For a description of the archeoseismological evidence we follow the nomenclature and classification after (Rodríguez-Pascua et al., 2011) and a careful comparison with other similar effects described in literature (Ferrater et al., 2015; Giner-Robles et al., 2009). We recorded the orientation and characteristics of each fracture measured in the Baths walls (i.e., dip azimuth and dip, sense of opening and aperture, presence of chipped corners and orientation of the wall where the fracture lies).

180

A high-resolution point cloud model of the Roman Baths has been obtained thanks to a Structure from Motion – Multi View Stereo workflow (e.g., Gallup et al., 2007; Goesele et al., 2007; Westoby et al., 2012).

185 We shot 1043 digital photos in RAW format with a reflex NIKON D5200 camera equipped with a 35 mm optical lens, allowing to minimize the lens distortions. We checked the internal accuracy of the model by means of 21 ground control points that were geotagged in the field and in the 3D model.

All the photos were processed with the Metashape Agisoft software, resulting in a highly accurate 3D point cloud, with an average spacing of 0.5 cm along the Baths walls.

The obtained dense point cloud was finally processed in the Cloud Compare software and in QGIS in order to extract
190 points included in narrow fences (profiles), remove outlier and interpolate in a mesh with a Delaunay Triangular Irregular Network (TIN) interpolation. Finally, values of dip and dip direction of each face of the interpolated mesh have been analyzed in a stereonet plot in order to detect subtle folding of originally horizontal reference surfaces.

3.3. GIS buffer analysis for source location

To provide a regional view, we compared the age of the studied earthquake-induced effects with other evidence known
195 in the Alpine area. To date, the best available database covering Holocene and historic time window is the Database of the Potential Paleoseismic Evidence in Switzerland (Kremer et al., 2020).

We listed all the evidence within a reasonable distance (i.e., 150 km) and considered as synchronous those evidence whose age (i.e., whenever the age of the event within a 2s confidence bound) overlap with the upper and lower age limits of the event recorded in Como. We here recall that the ages calculated in (Kremer et al., 2020) are based on age-depth
200 models with a linear interpolation between the closest dated samples and using an 'event corrected depth', i.e. on sediment depth subtracted from the thickness of sediment layers attributed to events (considered as 'instantaneous' layers relatively to the 'normal' background sedimentation).

In order back-calculate the paleo-magnitude and location of the possible seismogenic source that have triggered the described effects, we follow a grid search approach for inverting the distribution of sparse Intensity Data Points (IDPs).
205 As a preliminary step all the positive and negative evidence for a synchronous effect, triggered by the same earthquake, are collected. Then, lower and upper threshold Intensity values for triggering the considered effect are postulated: lower threshold values need to be exceeded at positive evidence locations; on the contrary, upper threshold values has to be not exceeded at negative sites.

The method consists of two steps: first all the locations with positive evidence are inverted in order to calculate the
210 Magnitude of the event that could have triggered the effect at increasing distances; then all locations with negative evidence are used to back-calculate the estimated local Intensity at those sites, given the results of the first step. Each grid cell where the back-calculated intensity exceeds the threshold is thus excluded.

Following the sensitivity analysis performed by Kremer et al. (2017), we solved the equations over an inverse grid search, by assuming an Intensity threshold value for mass wasting movement triggering of Intensity $VI_{2/10}$. Upper threshold
215 Intensity has been fixed at $VI_{5/10}$, allowing a certain degree of uncertainty due to the possible epistemic errors in associating positive or negative evidence for such old events.

During the first step, a grid-search approach calculates the moment magnitudes (Mw) over a grid of trial source locations (Bakun and Wentworth, 1997) using an empirical intensity attenuation relationship. We adopted the attenuation regression specifically developed by Fäh et al. (2011) for deep Alpine earthquakes, which has been already adopted in other similar

220 studies (Strasser et al., 2006, 2013; Kremer et al., 2017; Oswald et al., 2021).

For epicentral distances < 55 km:

$$I = -2.8941 + 1.7196 \, Mw - 0.03 \, D \qquad (1)$$

for epicentral distances > 55 km:

$$I = -4.2041 + 1.7196 \, Mw - 0.0064 \, D \qquad (2)$$

225 where I is the local Intensity (EMS98); Mw is the earthquake Moment Magnitude and D is the epicentral distance (km).

Each cell of the grid obtained from this process represents the Mw value of a hypothetical earthquake that is consistent with the triggering of the effects observed at all the positive locations.

During the second step of the analysis, the local Intensity values at the negative locations is back-calculated from the grid of the Magnitude values, allowing to exclude all those locations exceeding the upper threshold Intensity and thus resulting

230 in a more constrained area for the possible seismogenic source.

4. Results: evidence observed at Como city
4.1. Via Manzoni site

The Via Manzoni Site exposed a sequence of mainly fine-grained and fining-upward units down to the depth of 9 meters BGL; the relative position of the four investigated sections is presented in Figure 3a, while the composite stratigraphic

235 column is shown in Figure 4 ⌘. The stratigraphy from the ground level down to 3 meters BGL has not been documented but archeological observations constrain the age of that interval between the modern age and medieval times (Paul Blockley, *pers. comm.*).

Section 02FL records the stratigraphy between the depth of 3 and 6 meters BGL. It is composed of two fining-upward cycles from clast-supported gravels in sandy matrix to finely laminated fine sands alternating with silty loams rich in

240 biological remains. The depositional environment is an alluvial plain with overbank deposits alternating to fluvial channels and passing upward to a palustrine and lacustrine setting. Each cycle is relative to a progressive ingression of the shore and lacustrine environment onto the alluvial and fluvial one, due to a fast-subsiding setting, followed by episodes of alluvial aggradation by flooding events.

The base of the upper cycle is marked by laminated silty fine sands interested by fluidification and soft-sediment

245 deformation features (convolution features, above, and balls and pillow structures, below; Figure 4b and d) for a thickness of ca. 1 meter. These beds appear as entirely fluidized, and thus are interpreted as a single event of fluidization. The top of the fluidized interval lies below a pack of coarse gravels with load structures deforming the base of the gravels and both the underlying bed and the convoluted *laminae* as well (Figure 4d).

The sequence continues downwards with several cycles of fine beds alternating with coarse ones and with an overall

250 coarsening downward trend. Section 03 FL is partially overlapping and correlated with Section 03 PN, outcropping nearby and exposing 3 meters of slightly inclined beds (N34/16) and ascribable to the same depositional environment.

Section 03 PD is outcropping a few meters to the west of the FL one (Figure 3a). It exposes a sequence of foreset beds, moderately inclined toward the lake, bounded at the base and at the top by two unconformity surfaces and representing a progradation event of a lacustrine delta (Figure 4d). The top of the delta is correlative with the base of Section 02FL, as

255   confirmed and precisely defined by the dating.
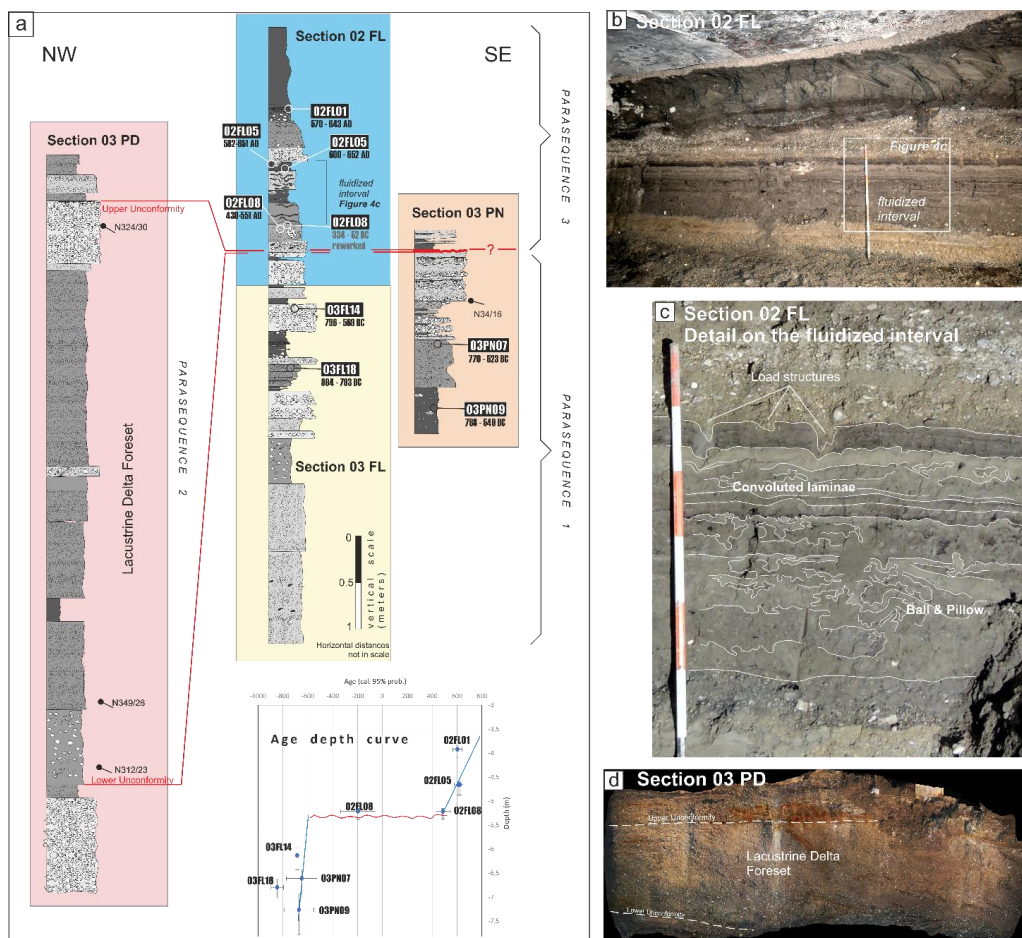
Figure 4: a) composite stratigraphic section for the Via Manzoni site: samples for ^{14}C dating and age results are reported (unit code in the black rectangles and calibrated ages with 95% prob.); see the Supplementary Material for a detailed Log; b) perspective on the 02FL Section and c) interpreted detail on the fluidized interval within the sequence; d) perspective on the 03PD Section, showing the two angular unconformities bounding a pack of lacustrine delta foreset beds.

The nine dated samples within the sequence (Table 1) allow to ascribe the entire documented stratigraphy to a period between the IX Cent. BC and the VII Cent. AD. The age-depth model (Figure 4) indicates that there is a major unconformity that can approximately be located at the depth of 5.20 meters BGL, that is close to the base of the fluidized

265   level. In this line, we were able to define three parasequences, composing the Via Manzoni stratigraphy. The base of the uppermost parasequence (Parasequence 3 in Figure 4) is marked by a maximum flooding surface that represents the

transition from aggradation (Parasequence 1) to regression in the system, due to the ongoing subsidence of the Como basin. The hiatus at the maximum flooding surface is laterally corresponding to the growth of the lacustrine delta (Parasequence 2), that can be consistently ascribable to a period between ca. VII Cent. BC and the V-VI Cent. AD, even if lacking direct dating.

From the evidence above, we can finally assess that i) the fluidization observed in Section 02FL is triggered by ground shaking and ii) the event is chronologically constrained at the passage between the VI and VII Cent. AD, most probably at the end of the VI Cent. AD. Lower age bound comes from the minimum age of the 02FL08 sample dating, i.e., the lowermost deformed unit, whereas upper age bound is given by the maximum age of 02FL05 sample. If we consider these constraints, we obtain a possible event age of 430 – 652 cal yr AD. Nonetheless, a more constrained age is estimated by considering the inner bounds from the age coming from datings: i.e., 551 – 582 cal yr AD. This age constrain comes from the assumption that the whole fluidized interval has been deformed by a single event.

Unit	Lab. code	Start Weigth (mg)	Cellulose (mg)	^{14}C age (yr. BP)	Calibrated age – yr (prob. 95%)	Depth (m) (middle point of the layer; * exact depth)
02FL01	BRA5514	45,5	4,27	1467±21	570-643 AD	-3,90
02FL05	BRA6056	67,9	5,4	1445±24	582-651 AD	-4,64
02FL05	BRA5502	78,2	13,7	1426±20	600-652 AD	-4,64
02FL08	BRA5515	87,1	4,9	1573±19	430-551 AD	-5,20
02FL08	BRA5504	86	17,2	2116±21	334-52 BC	-5,20
03FL14	BRA5517	83,5	9,7	2550±22	796-569 BC	-6,12 *
03FL18	BRA5518	75,9	3,6	2656±23	894-793 BC	-6,79 *
03PN07	BRA5510	75,5	7,9	2488±22	770-523 BC	-6,60
03PN09	BRA5519	80,4	11	2529±22	788-549 BC	-7,26

Table 1: dating results; the 14C age and calibrated age (with an associated accuracy of 95%) is reported, together with the sampling depth; the 14C ages were calibrated using IntCal20 calibration curve in OxCal 4.4 program (Ramsey, 2009; Reimer et al., 2020).

4.2. Roman Baths site

The Roman Baths preserve some peculiar damages on the walls and structures that can be interpreted as Earthquake Archeological Effects (EAEs, *sensu* Rodríguez-Pascua et al., 2011; Figure 5).

A preserved arch shows evidence of partial collapse (Figure 5b) and stone movements, possibly caused by the repeated shaking of non-collapsed walls. An entire wall section, that was presumably originally placed at ca. 2 m of height, is presently sticking out of the ground, in vertical position, right next to its original location (Figure 5c). The wall collapsed onto a layer of alluvial sediments that were deposited at the site after its definitive abandonment, most probably when the V-VI Cent. AD tombs have been excavated at the site.

Building stones are affected by several corner chips and fractures which either crosscut single stones or pervasively run across entire walls. We measured 205 fractures in the site including features cutting through the stones and the mortar, recording the orientation of fracture at chipped corners and the aperture of the fractures as well. Widening downward fractures are particularly indicative for archaeoseismology since these are hardly caused by differential compaction of soil. Fracture orientation (Figure 6) indicates that the most frequent strike orientations are N30 and N110, with a secondary prevalence of N90 and N170 striking fractures. These directions are oblique to those ones of the Baths walls (i.e., N80 and N170), allowing to exclude that the observed damages are mainly due to the walls' settlement through time.

A section of the walls showed evidence for very subtle folding and of restoring interventions through time. The stone rows, at this site, are irregular; an additional row of stones has been added at the beginning of the second building phase. The analysis of the high-resolution 3D models of the baths allowed to extract a mesh model for each stone row and to analyze subtle folding and deformations (Figure 6e and f). We observe that the wall is gently folded along an antiform with a subvertical axial plane striking ca. NE-SW, consistently with the strike of the main fracture sets we measured.
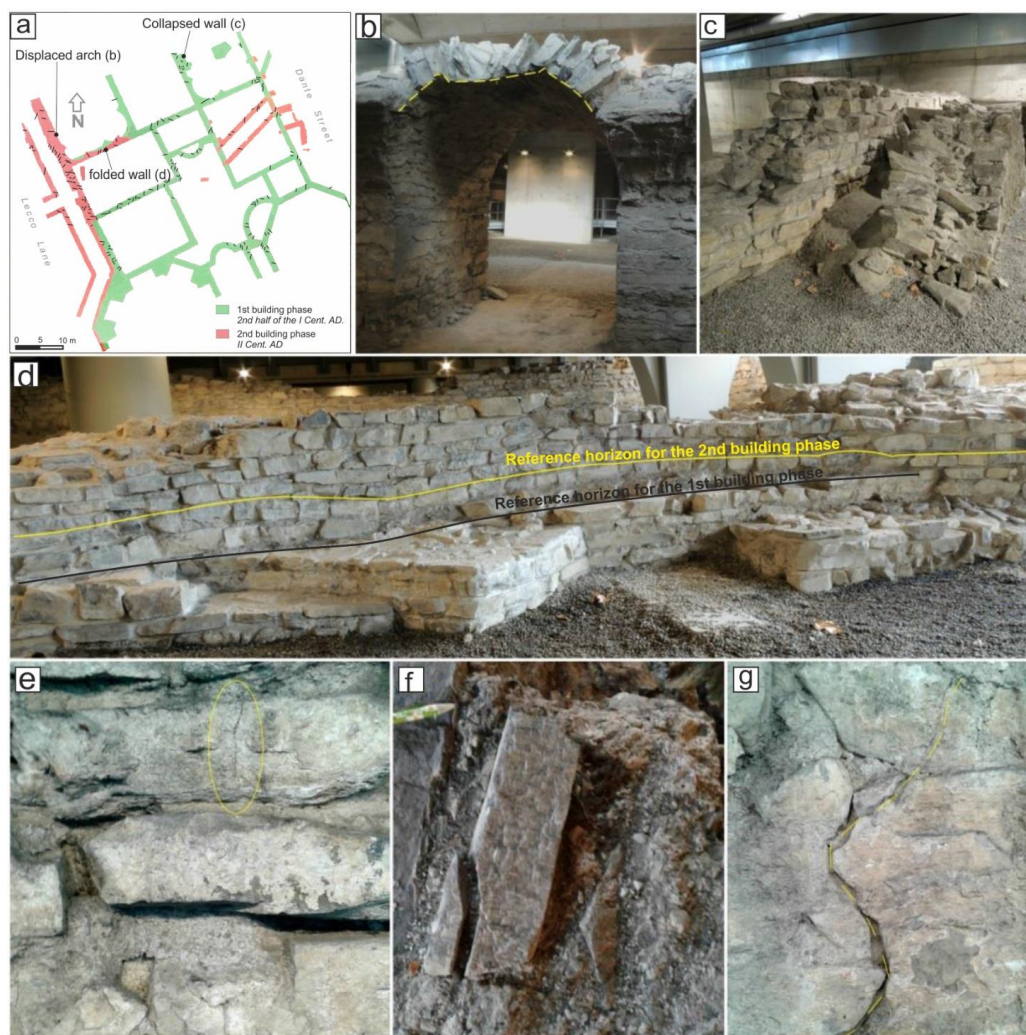
Figure 5: Potential Earthquake-induced Archeoseismological Effects surveyed at the Como Roman Baths: a) b) collapsed arch with displaced stones; c) collapsed wall, view from the east; d) a well-preserved section of the walls showing very subtle evidence of folding: a line of stones showing the loss of horizontality has been highlighted; e) fractures in single stone blocks; f) chipped corners; g) penetrative fractures cutting through the stones and the mortar.

305
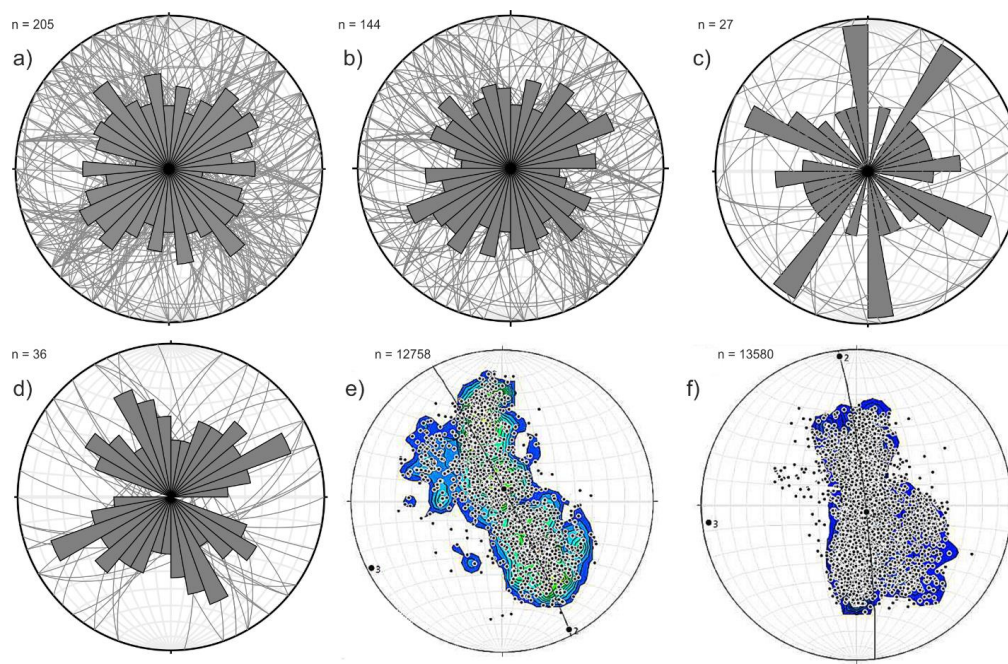
310 **Figure 6: stereoplot and rose diagram (directions) of the fractures measured at the Como Roman Baths: a) all fractures; b) fractures in stone and mortar; c) chipped corners; d) widening-downward fractures; e) facets orientation extracted from the mesh of a single row of stones belonging to the 1st building phase; f) same data for a row belonging to the 2nd building phase.**

5. Discussion
5.1. Footprint of the VI Cent. AD event

315   The investigations at Como downtown allow to identify the occurrence of at least one paleoseismic event that triggered the effects observed and described at Como City: we will refer hereafter to this ancient earthquake as the VI Cent. AD Event. The lack of any historical account for such an event prevents any investigation in this sense; nonetheless it is reasonable that the shaking of the same earthquake could have produced similar effects in other sites, where the geological and geomorphological setting is particularly sensible to earthquake-induced secondary effects. Previously, studies on the

320   lacustrine stratigraphic records in the Alps as natural "seismometers" (e.g., Oswald et al., 2021; Strasser et al., 2006, 2013) offered consistent results for historical earthquakes and opened the possibility to quantitively explore the occurrence of prehistorical events.

We evaluate this hypothesis by incorporating in our analysis surrounding sites that present positive and negative evidence; we considered the Swiss database (Kremer et al., 2020), supplemented with more recent publications (e.g., Nigg et al.,

325   2021; Rapuc et al., 2022). The location of the sites is presented in Figure 7, while Table 2 presents a summary of the available information for positive evidence.

Lake sediments acts as natural seismographs, since that may archive information on seismic shaking occurred in the past (Strasser et al., 2013); the stratigraphy of lake sediments can be investigated using high-resolution geophysical surveys, often supplemented by core drillings, to ground-truth seismic data and to recover datable material. Mass-transport deposits

330 (MTDs) are easily recognized in seismic data due to their chaotic facies, in stark contrast to the regularly laminated undisturbed sediments.

Extensive investigations have been performed in the northern side of the Alps (e.g., Monecke et al., 2006; Strasser et al., 2006, 2013; Beck, 2009); a dataset of paleoseismic evidence in Switzerland and conterminous regions has been recently presented by Kremer et al. (2020). Paleoseismic evidence is not randomly distributed through time but is clustered at

335 specific dates; in particular, enhanced seismic activity is documented at ca. 9700, 6500 and in the last 4000 cal yr BP (Strasser et al., 2013; Kremer et al., 2020).

The southern side of the Alps has been investigated less systematically; nevertheless, some studies identified turbidites in lake deposits. Such MTDs have been tentatively associated with seismic shaking.

Fanetti et al. (2008) performed limno-geological investigations in Lake Como, including a bathymetric survey, high-

340 resolution seismic reflection studies and gravity cores analyses. They identified two megaturbidite bodies, up to 3.5 m thick, interpreted as the result of large debris flows originated from the northern part of the Lake Como branch. The oldest deposit has a volume of ca. $10 \cdot 10^6$ m^3, while the upper deposit has a volume of $3 \cdot 10^6$ m^3. Chronological constraints are not well-substantiated, but extrapolation of mean sedimentation rates obtained from ^{137}Cs and ^{14}C dating allow to infer a tentative age of 6th and 12th Century AD for the two deposits.

345 In Lake Iseo, sediments were retrieved from the Sale Marasino sub-basin (Lauterbach et al., 2012) and from the main, deeper basin (Rapuc et al., 2022). In both cases, detrital event layers with metric thickness were identified and possibly related to seismic shaking. Rapuc et al. (2022) used geochemical proxies to distinguish extreme flood events from sediments accumulation driven by destabilization of slopes and delta. One event layer fits with the time frame of interest for our research: it is represented by a 1.4 m thick deposit, dated at 640-830 AD.

350 In Lake Garda, two major MTD beds were identified in the seismic stratigraphy, representing more than 50% of the Holocene sedimentary record in the lake depocenter (Gasperini et al., 2020). Although the chronological constraints are highly speculative, one MTD layer is tentatively related to onshore evidence of surface faulting during the mid-III century AD at an archaeological site at Egna (Adige Valley; Galadini & Galli, 1999).

In Lake Sils (Upper Engadine), an up to 6 m thick turbidite has been identified, with an estimated volume of 6.5 million

355 m^3; the top of the deposit is dated at 650-780 AD (Blass et al., 2005), while the peat layer underlying the event deposit is dated at 225-419 AD (Nigg et al., 2021). The megaturbidite extends over the entire lake and is interpreted as the result of a sudden collapse of the main delta entering the lake; it generated tsunami waves up to 5 m high, which inundated the lakeshore (Nigg et al., 2021).

Two sedimentary cores were retrieved from Lake Alzasca (Ticino region, Switzerland) and analyzed to reconstruct the

360 flood history. A complete Holocene succession was obtained, and the chronological constraints are supported by nine ^{14}C ages (Wirth, 2013). Two events listed by Kremer et al. (2020) overlap with the paleoseismic evidence dated at Como; their timing is derived from the nearest dated samples and the age-depth curve (Table 2).

A similar situation holds for Lake Cadagno (Ticino region, Switzerland), where two Holocene sediment successions were recovered from the deeper part of the basin. Nine ^{14}C dated samples provide chronological constraints to reconstruct the

365 flood history (Wirth, 2013). Two events listed by Kremer et al. (2020) overlap with the paleoseismic evidence dated at Como.

Available data for Lake Lungern include a dense grid of high-resolution seismic lines and sedimentary cores (Monecke et al., 2006). A total of 19 dated samples are used to derive an age-depth curve, which goes back up to about 2000 yr BP; three of the deformation horizons identified at Lake Lungern (LNG4, 5 and 6) have an age overlapping with the event

370 dated at Como.

Knapp et al. (2018) apply sedimentology, radiocarbon dating and geophysics to investigate Lake Oeschinen (Swiss Alps). They found evidence of eleven rock-slope failure events, which in four cases have been related to (pre)-historic earthquakes. Radiocarbon dating allowed to reconstruct the local evolution in the last 2500 years; one of the events identified in Lake Oeschinen overlaps with the paleoseismic evidence at Como.

375 Table 2 includes also two entries from Lake Engstlen and Lake Hinterburgsee; these data are less constrained than other lakes, due to unclear dating or stratigraphic interpretation (Katrina Kremer, personal communication).

Locality	Distance from Como (km)	Dates of the synchronous events (cal yr prob 95%)	Reference	Notes
Lake Como	15	500-600 AD	Fanetti et al., 2008	Date extrapolated
Lake Alzasca	63	633-816 AD	Wirth, 2013	offset from nearest dated sample: ~210y
Lake Alzasca	63	513-688 AD	Wirth, 2013	offset from nearest dated sample: ~90y
Lake Iseo	80	640-830 AD	Rapuc et al., 2022	
Lake Sils	84	650-780 AD	Nigg et al., 2021	
Lake Cadagno	87	579-963 AD	Wirth, 2013	offset from nearest dated sample: ~0y
Lake Cadagno	87	619-1006 AD	Wirth, 2013	offset from nearest dated sample: ~40y
Lake Engstlen	121	650-918 AD	Kremer et al., 2020	offset from nearest dated sample: ~230y, and uncertainties in composing the master core. Dating is not fully reliable (Kremer, *pers. comm.*)
Lake Hinterburgsee	128	644 AD	Wirth, 2013	offset from nearest dated sample: ~50y (the evidence is unclear; Kremer, *pers. comm.*)
Lake Oeschinen	130	580-680 AD	Knapp et al., 2018	
Lake Lungern	131	360-620 AD	Monecke et al., 2006	offset from nearest dated sample in composite core: 5y
Lake Lungern	131	380-800 AD	Monecke et al., 2006	turbidite and mass flow on seismic reflection
Lake Lungern	131	520-730 AD	Monecke et al., 2006	offset from nearest dated sample in composite core: 50y

Table 2: summary of the positive evidence; see locations in Figure 7.
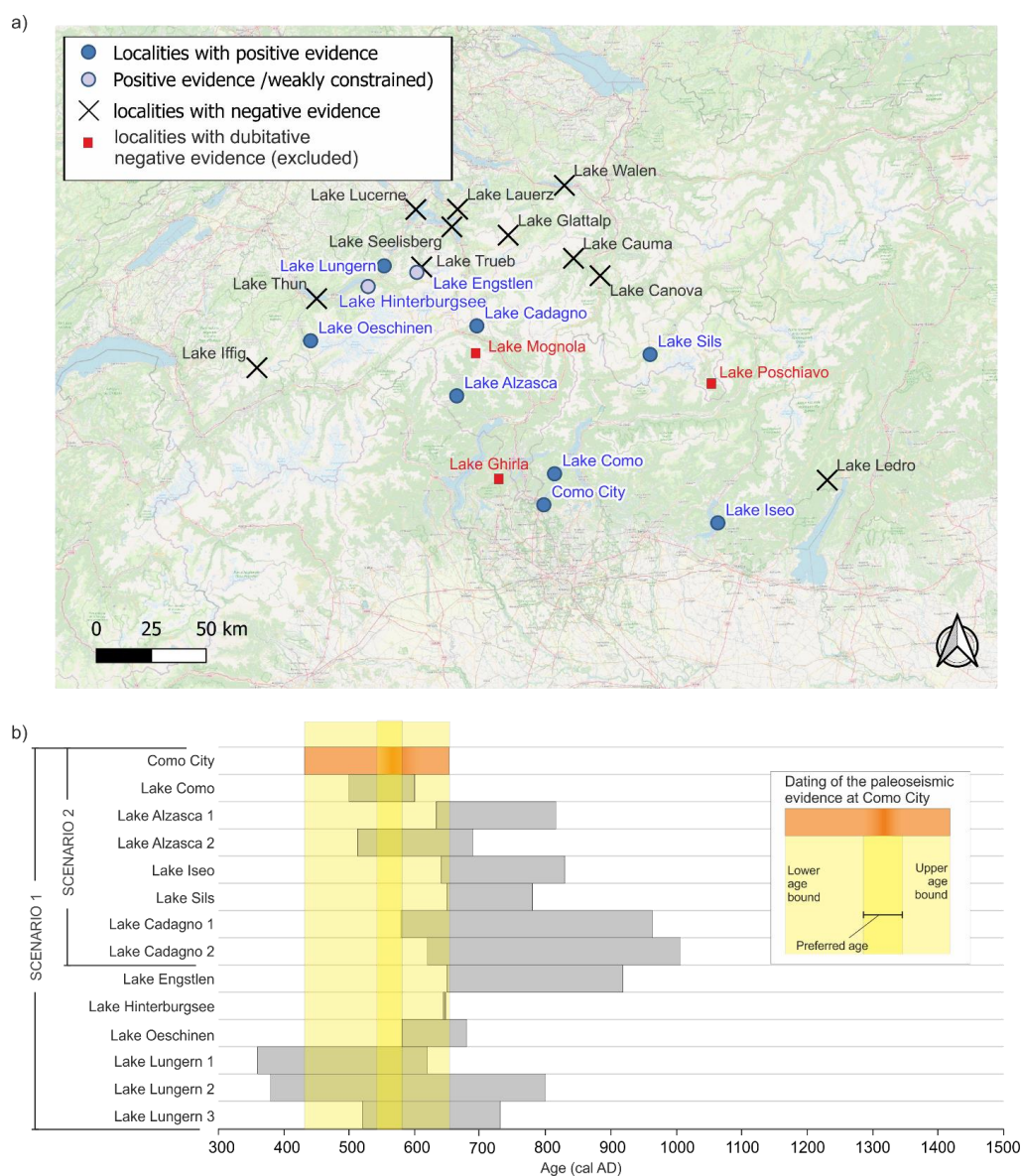
Figure 7: a) localities with positive and negative evidence for a synchronous effect caused by the VI Cent. AD earthquake (after the database available in Kremer et al., 2020), some of the localities have been excluded (red squares) due to incomplete stratigraphy or dubitative evidence (see the text for details); basemap after © OpenStreetMap contributors 2023. Distributed under the Open Data Commons Open Database License (ODbL) v1.0.; **b)** a comparison of the dated evidence at Como City with the age constraint for all the possible positive evidence of synchronous turbidites the Alpine lakes; age limits are given by the upper and lower boundary of the event age, given the age-depth curve calculated for any site and considering 2s of confidence interval (data after Kremer et al., (2020) and available under request to the Authors).

Figure 7b shows the age overlap among multiple sites, ordered according to their distance from the Como City site. Blue dots represent positive evidence, whereas crosses indicate localities of negative evidence.

All the positive evidence overlaps with the upper and lower age limits for the paleo-earthquake (Figure 7b). If we consider
390   a narrower time interval for the age of the paleo-earthquake (i.e., within the max. age of the lower limit and the min. age of the upper limit), the overlapping events indicate a limited number of localities to be correlated (e.g., Lake Como, Lake Alzasca, Lake Oeschinen and Lake Lungern) but still the distribution of these lakes overlaps with a more inclusive scenario. As mentioned before, Lake Englsten and Lake Hinterburgsee suffer from higher uncertainty.

Some of the localities (red squares in Figure 7) have been excluded due to their incomplete stratigraphy or to dubitative
395   evidence. These are: Lake Mognola, Lake Ghirla and Lake Poschiavo.

At Lake Ghirla, located close to the City of Como, there are no events listed by Kremer et al. (2020) as possibly synchronous to the VI Cent. AD event. The stratigraphy of Lake Ghirla is well constrained by datings and records continuously a time window extending back to 13 Ka BP (Wirth, 2013) with a dating located close to the time interval of interest. Nonetheless, a single episode of sedimentation with high detrital content is recorded close to the age of the paleo-
400   earthquake, possibly constituting a positive evidence for such a small lake with a limited catchment. We thus found ambiguous evidence for this small lake and preferred to exclude it from any further analysis.

Lake Mognola is a small lake with a limited catchment as well. Its stratigraphic record, analyzed by Wirth (2013) for paleoclimate reconstructions, presents a peculiar stratigraphic record, not comparable with any other lake of the Southern Alps, that lead to the exclusion of this lake from further analyses. Possibly, these peculiarities emerge from the relatively
405   high altitude of the site (2003 m asl) dominated by clastic and glacial geomorphologic processes. We thus excluded the site from our analysis as well.

Finally, Lake Poschiavo is characterized by very high sedimentation rates and possibly the available stratigraphic record is not reaching the requested time window.

5.2. Potential source location

410   In the following analysis, we'll perform our calculations on two different datasets of positive evidence (Figure 7b), resulting in two output scenarios (Figure 8).

In Scenario 1 we used all the possible locations reporting positive evidence synchronous with the VI Cent. AD event; in Scenario 2 we excluded the locations in the Swiss Alps, due to i) their vicinity with other localities showing negative evidence instead, ii) the reported uncertainties and limited overlap of the dated events from Lake Engstlen and Lake
415   Hinterburgsee, and iii) the vicinity of other seismogenic sources (e.g., Fritsche et al., 2012; Strasser et al., 2013) that could be more probably invoked as sources for mass wasting events in this area.

The inversion of the locations with positive and negative evidence of a paleo-earthquake synchronous with the VI Cent. AD event indicates a possible source located in the Southern Alps or close to the Periadriatic Line (Figure 8). The minimum of the calculated earthquake magnitude is Mw 6.32, if we consider Scenario 2; in Scenario 1 the minimum
420   magnitude is increased to Mw 6.43. Both the scenarios, when considered with the constraints of the negative evidence locations, point to a similar area where the possible seismogenic source would have been located.

The area encompassing the minimum estimated Mw values (ca. Mw 6.4 – 6.5) are likely connected with the Tonale Line or other structures located close to the Italy-Switzerland border (Figure 8b). Another possible candidate as a seismogenic source is the Gonfolite Backthrust (GB in Figure 8b), with a possible associated Mw of ca. 6.4: this fault has already been
425 identified as potentially active (Michetti et al., 2012; Sileo et al., 2007).

Other possible sources should be located more to the south, associated with a higher magnitude range (Mw 6.6 – 6.7). This scenario seems less likely, due to the absence of known active faults in the area. We underline that the lack of negative evidence to the south could be possibly ascribed to the lack of studies and stratigraphic records in the Po Plain sector.

a) **Positive evidence only**
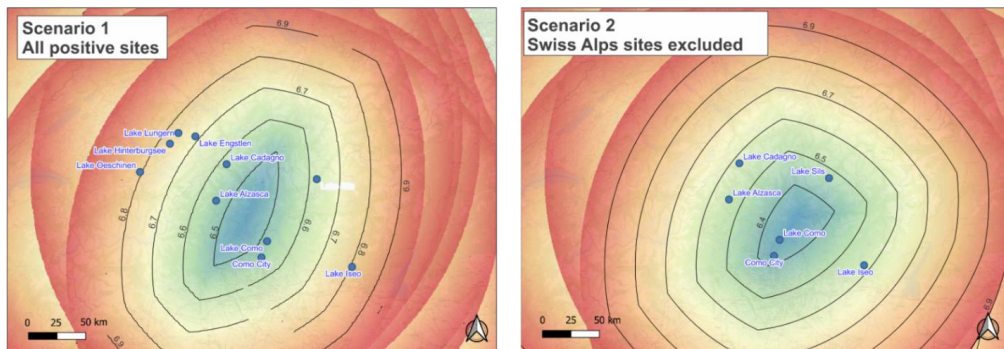
b) **Positive and negative evidence**
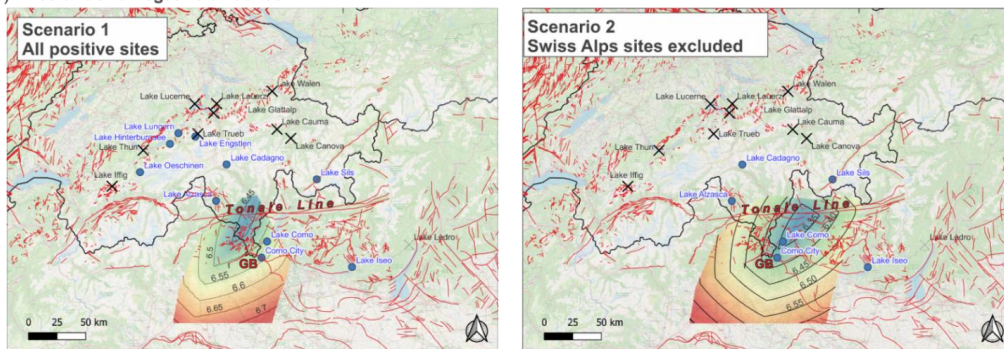
430

Figure 8: results from the inverse grid search of the paleo-earthquake, considering two possible Scenarios of positive evidence (see text for details): a) only positive evidence included; b) positive and negative evidence included with a map of the potentially active faults of Switzerland (after Hetenyi et al., 2018) and Capable Faults for Italy; after Guerrieri et al., 2015; GB, Gonfolite Backthrust). All basemaps after © OpenStreetMap contributors 2023. Distributed under the Open Data Commons Open
435 **Database License (ODbL) v1.0.**

6. Conclusions

The main conclusions of this study can be summarized as follows:

- We found deformations in a stratigraphic sequence and in an archaeological site in Como city, dated at the VI century AD. We interpret such deformations as evidence of earthquake ground shaking.
- We gathered information from published literature for other sites in the Western Southern Alps where paleoseismic evidence has been inferred in the same time interval.
- By applying an inverse-grid approach, we claim that a so far undocumented earthquake (minimum Mw 6.32) with epicentral location at the border between Italy and Switzerland can explain the spatial pattern and distribution of paleoseismic evidence dated at the VI century AD.
- Our study prompts for the need to better evaluate the seismic risk in the Western Southern Alps, a low-deforming region characterized by high density of infrastructures and economical assets.

Author contribution

FAL and EM collected the samples, described the stratigraphic sections and documented all the excavations and the Via Manzoni Site; FAL built the virtual 3D model of the Roman Baths and analyzed the archeoseismological evidence with MFF; ST and SC analyzed and treated all the samples for datings; FAL inverted the intensity datapoints for source location and magnitude calculations; AMM supervised the research and reviewed the manuscript; FL prepared the manuscript with contributions from all co-authors.

Competing Interests

The authors declare that they have no conflict of interest.

Acknowledgements

Katrina Kremer is acknowledged for having provided, under request, the dataset after Kremer et al (2017) and for fruitful discussion; The Authors are indebted to the SABAP (Soprintendenza Archeologia, Belle Arti e Paesaggio) of the Como. Graduate M.Sc. Dr. Elisa Ticozzi, Dr. Federica Cozzula and B.sc. Dr. Camilla Clerici and particularly thanked for having provided their time and effort and contributing to this research: part of the results of this paper are the fruit of the results discussed in their theses.

References

Borgatti, L. and Soldati, M.: Landslides as a geomorphological proxy for climate change: a record from the Dolomites (northern Italy), Geomorphology, 120, 56–64, 2010.

Casini, S.: Carta archeologica della Lombardia: La Provincia di Como., FC Panini Editore, 1994.

Castellarin, A., Vai, G. B., and Cantelli, L.: The Alpine evolution of the Southern Alps around the Giudicarie faults: A Late Cretaceous to Early Eocene transfer zone, Tectonophysics, 414, 203–223, https://doi.org/10.1016/j.tecto.2005.10.019, 2006.

Castelletti, L. and Motella De Carlo, S.: Il fuoco e la montagna. Archeologia del Paesaggio dal Neolitico all'Età Moderna in alta Val Cavargna, Castelletti, Lanfredo; Motella De Carlo, Sila, Como, 209 pp., 2012.

Cercatillo, S., Friedrich, M., Kromer, B., Paleček, D., and Talamo, S.: Exploring different methods of cellulose extraction for 14 C dating, New Journal of Chemistry, 45, 8936–8941, 2021.

475   Comerci, V., Capelletti, S., Michetti, A. M., Rossi, S., Serva, L., and Vittori, E.: Land subsidence and Late Glacial environmental evolution of the Como urban area (Northern Italy), Quaternary International, 173, 67–86, 2007.

Cremaschi, M.: Manuale di geoarcheologia, Laterza, 2000.

Fäh, D., Giardini, D., Kästli, P., Deichmann, N., Gisler, M., Schwarz-Zanetti, G., Alvarez-Rubio, S., Sellami, S., Edwards, B., and Allmann, B.: ECOS-09 earthquake catalogue of Switzerland release 2011 report and database. Public
480   catalogue, 17. 4. 2011. Swiss Seismological Service ETH Zurich, RISK, 2011.

Fanetti, D., Anselmetti, F. S., Chapron, E., Sturm, M., and Vezzoli, L.: Megaturbidite deposits in the Holocene basin fill of Lake Como (Southern Alps, Italy), Palaeogeography, Palaeoclimatology, Palaeoecology, 259, 323–340, https://doi.org/10.1016/j.palaeo.2007.10.014, 2008.

Fantoni, R., Bersezio, R., and Forcella, F.: Alpine structure and deformation chronology at the Southern Alps-Po Plain
485   border in Lombardy, Bollettino della Società geologica italiana, 123, 463–476, 2004.

Ferrario, M. F., Brunamonte, F., Caccia, A., Livio, F., Martinelli, E., Mazzola, E., Michetti, A. M., and Terrana, S.: Buried landscapes: geoarchaeology of the roman harbor of Como (N Italy), Alp. Mediterr. Quat, 28, 2015.

Ferrater, M., Silva, P. G., Ortuño, M., Rodríguez-Pascua, M. Á., and Masana, E.: Archaeoseismological analysis of a Late Bronze Age site on the Alhama de Murcia fault, SE Spain, Geoarchaeology, 30, 151–164, 2015.

490   Fritsche, S., Fäh, D., and Schwarz-Zanetti, G.: Historical intensity VIII earthquakes along the Rhone valley (Valais, Switzerland): primary and secondary effects, Swiss J Geosci, 105, 1–18, https://doi.org/10.1007/s00015-012-0095-3, 2012.

Gallup, D., Frahm, J.-M., Mordohai, P., Yang, Q., and Pollefeys, M.: Real-time plane-sweeping stereo with multiple sweeping directions, in: 2007 IEEE Conference on Computer Vision and Pattern Recognition, 1–8, 2007.

495   Giner-Robles, J. L., Rodríguez-Pascua, M. A., Pérez-López, R., Silva, P. G., Bardají, T., Grützner, C., and Reicherter, K.: Structural analysis of earthquake archaeological effects (EAE): Baelo Claudia examples (Cádiz, South Spain), Instituto Geológico y Minero de España, 2009.

Goesele, M., Snavely, N., Curless, B., Hoppe, H., and Seitz, S. M.: Multi-view stereo for community photo collections, in: 2007 IEEE 11th International Conference on Computer Vision, 1–8, 2007.

500   Guerrieri, L., Blumetti, A. M., Comerci, V., Manna, P. D., Michetti, A. M., Vittori, E., and Serva, L.: Surface Faulting Hazard in Italy: Towards a First Assessment Based on the ITHACA Database, in: Engineering Geology for Society and Territory - Volume 5, Cham, 1021–1025, https://doi.org/10.1007/978-3-319-09048-1_195, 2015.

Guidoboni, E., Comastri, A., and Phillips, B.: Catalogue of Earthquakes and Tsunamis in the Mediterranean Area from the 11th to the 15th Century, Istituto nazionale di geofisica e vulcanologia Rome, Italy, 2005.

505   Handy, M. R., Schmid, S. M., Bousquet, R., Kissling, E., and Bernoulli, D.: Reconciling plate-tectonic reconstructions of Alpine Tethys with the geological–geophysical record of spreading and subduction in the Alps, Earth-Science Reviews, 102, 121–158, 2010.

ISIDe Working Group: Italian seismological instrumental and parametric database (ISIDe), 2007.

Jorio, S.: Le terme di Como romana: seconda metà I-fine III secolo dC; testi dei pannelli didattici, Ed. Et, 2011.

510   Knapp, S., Gilli, A., Anselmetti, F. S., Krautblatter, M., and Hajdas, I.: Multistage rock-slope failures revealed in lake sediments in a seismically active Alpine region (Lake Oeschinen, Switzerland), Journal of Geophysical Research: Earth Surface, 123, 658–677, 2018.

Kremer, K., Wirth, S. B., Reusch, A., Fäh, D., Bellwald, B., Anselmetti, F. S., Girardclos, S., and Strasser, M.: Lake-sediment based paleoseismology: Limitations and perspectives from the Swiss Alps, Quaternary Science Reviews, 168,
515   1–18, https://doi.org/10.1016/j.quascirev.2017.04.026, 2017.

Kremer, K., Gassner-Stamm, G., Grolimund, R., Wirth, S. B., Strasser, M., and Fäh, D.: A database of potential paleoseismic evidence in Switzerland, J Seismol, 24, 247–262, https://doi.org/10.1007/s10950-020-09908-5, 2020.

Luraschi, G.: Storia di Como antica: saggi di archeologia, diritto e storia, New Press, 1997.

520   Martinelli, E., Michetti, A. M., Colombaroli, D., Mazzola, E., Motella De Carlo, S., Livio, F., Gilli, A., Ferrario, M. F., Höbig, N., Brunamonte, F., Castelletti, L., and Tinner, W.: Climatic and anthropogenic forcing of prehistorical vegetation succession and fire dynamics in the Lago di Como area (N-Italy, Insubria), Quaternary Science Reviews, 161, 45–67, https://doi.org/10.1016/j.quascirev.2017.01.023, 2017.

Martinelli, E., Michetti, A. M., Castelletti, L., Colombaroli, D., Ferrario, M. F., Livio, F. A., Motella De Carlo, S., and Tinner, W.: Il paesaggio preromano proto-urbano nei dintorni di Como: contesto ambientale e trasformazioni 525   antropiche., Scenari di ricostruzione delle interazioni uomo-ambiente in Lombardia (N-Italia) dal Paleolitico medio all'età del Ferro., Firenze, 9–36, 2022.

Michetti, A., Giardina, F., Livio, F., Mueller, K., Serva, L., Sileo, G., Vittori, E., Devoti, R., Riguzzi, F., and Carcano, C.: Active compressional tectonics, Quaternary capable faults, and the seismic landscape of the Po Plain (N Italy), Annals of geophysics, 2012.

530   Michetti, A. M., Livio, F. A., Pasquarè, F., Aligi, Vezzoli, L., Bini, A., Bernoulli, D., and Sciunnach, D.: Carta Geologica d'Italia, Foglio 075, Como, 2014.

Monecke, K., Anselmetti, F. S., Becker, A., Schnellmann, M., Sturm, M., and Giardini, D.: Earthquake-induced deformation structures in lake deposits: A Late Pleistocene to Holocene paleoseismic record for Central Switzerland, Eclogae Geologicae Helvetiae, 99, 343–362, 2006.

535   Oswald, P., Strasser, M., Hammerl, C., and Moernaut, J.: Seismic control of large prehistoric rockslides in the Eastern Alps, Nat Commun, 12, 1059, https://doi.org/10.1038/s41467-021-21327-9, 2021.

Ramsey, C. B.: Bayesian analysis of radiocarbon dates, Radiocarbon, 51, 337–360, 2009.

Reimer, P. J., Austin, W. E. N., Bard, E., Bayliss, A., Blackwell, P. G., Ramsey, C. B., Butzin, M., Cheng, H., Edwards, R. L., Friedrich, M., Grootes, P. M., Guilderson, T. P., Hajdas, I., Heaton, T. J., Hogg, A. G., Hughen, K. A., Kromer, 540   B., Manning, S. W., Muscheler, R., Palmer, J. G., Pearson, C., Plicht, J. van der, Reimer, R. W., Richards, D. A., Scott, E. M., Southon, J. R., Turney, C. S. M., Wacker, L., Adolphi, F., Büntgen, U., Capano, M., Fahrni, S. M., Fogtmann-Schulz, A., Friedrich, R., Köhler, P., Kudsk, S., Miyake, F., Olsen, J., Reinig, F., Sakamoto, M., Sookdeo, A., and Talamo, S.: The IntCal20 Northern Hemisphere Radiocarbon Age Calibration Curve (0–55 cal kBP), Radiocarbon, 62, 725–757, https://doi.org/10.1017/RDC.2020.41, 2020.

545   Rodríguez-Pascua, M. A., Pérez-López, R., Giner-Robles, J. L., Silva, P. G., Garduño-Monroy, V. H., and Reicherter, K.: A comprehensive classification of Earthquake Archaeological Effects (EAE) in archaeoseismology: Application to ancient remains of Roman and Mesoamerican cultures, Quaternary International, 242, 20–30, 2011.

Rotondi, R. and Garavaglia, E.: Statistical analysis of the completeness of a seismic catalogue, Natural Hazards, 25, 245–258, 2002.

550   Rovida, A., Locati, M., Camassi, R., Lolli, B., and Gasperini, P.: Catalogo Parametrico dei Terremoti Italiani, versione CPTI15, release 1.5, 33, https://doi.org/10.6092/INGV.IT-CPTI15, 2016.

Scaramuzzo, E., Livio, F. A., Granado, P., Di Capua, A., and Bitonte, R.: Anatomy and kinematic evolution of an ancient passive margin involved into an orogenic wedge (Western Southern Alps, Varese area, Italy and Switzerland), Swiss J Geosci, 115, 4, https://doi.org/10.1186/s00015-021-00404-7, 2022.

555   Schmid, S. M. and Kissling, E.: The arc of the western Alps in the light of geophysical data on deep crustal structure, Tectonics, 19, 62–85, https://doi.org/10.1029/1999TC900057, 2000.

Sileo, G., Giardina, F., Livio, F., Michetti, A. M., Mueller, K., and Vittori, E.: Remarks on the Quaternary tectonics of the Insubria Region (Lombardia, NW Italy, and Ticino, SE Switzerland), BOLLETTINO-SOCIETA GEOLOGICA ITALIANA, 126, 411, 2007.

560   Strasser, M., Anselmetti, F. S., Fäh, D., Giardini, D., and Schnellmann, M.: Magnitudes and source areas of large prehistoric northern Alpine earthquakes revealed by slope failures in lakes, Geology, 34, 1005–1008, https://doi.org/10.1130/G22784A.1, 2006.

Strasser, M., Monecke, K., Schnellmann, M., and Anselmetti, F. S.: Lake sediments as natural seismographs: A compiled record of Late Quaternary earthquakes in Central Switzerland and its implication for Alpine deformation,
565   Sedimentology, 60, 319–341, https://doi.org/10.1111/sed.12003, 2013.

Stucchi, M., Albini, P., Mirto, M., and Rebez, A.: Assessing the completeness of Italian historical earthquake data, Annals of Geophysics, 2004.

Trauth, M. H., Bookhagen, B., Marwan, N., and Strecker, M. R.: Multiple landslide clusters record Quaternary climate changes in the northwestern Argentine Andes, Palaeogeography, Palaeoclimatology, Palaeoecology, 194, 109–121,
570   https://doi.org/10.1016/S0031-0182(03)00273-6, 2003.

Uboldi, M.: Carta archeologica della Lombardia, Como. La città murata e la convalle. Franco Cosimo Panini, Modena, 1993.

Westoby, M. J., Brasington, J., Glasser, N. F., Hambrey, M. J., and Reynolds, J. M.: 'Structure-from-Motion'photogrammetry: A low-cost, effective tool for geoscience applications, Geomorphology, 179, 300–314, 2012.

575   Wirth, S. B.: The Holocene flood history of the central Alps reconstructed from lacustrine sediments: frequency, intensity and controlling climate factors - PhD Thesis, ETH Zurich, 2013.

Zanchetta, S., Malusà, M. G., and Zanchi, A. M.: Precollisional development and Cenozoic evolution of the Southalpine retrobelt (European Alps), Lithosphere, L466.1, https://doi.org/10.1130/L466.1, 2015.